Laboratoř růstových regulátorů

Miroslav Strnad

Kyselina abscisová
[kap. 23]

- Univerzita Palackého & Ústav experimentální botaniky AV CR

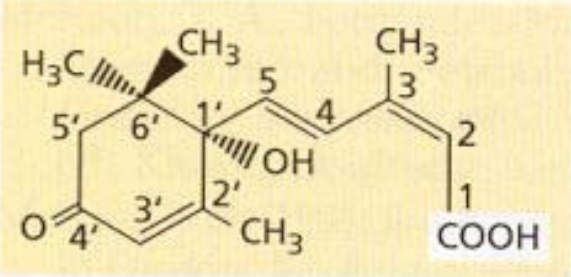

(*S*)-*cis*-ABA (naturally occurring active form)

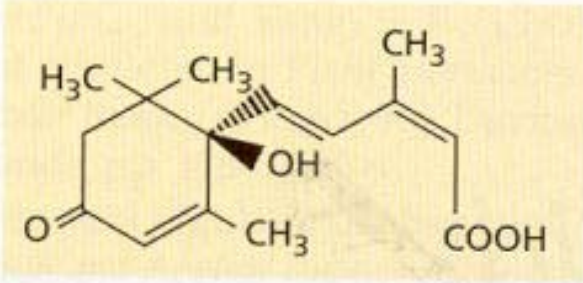

(*R*)-*cis*-ABA (inactive in stomatal closure)

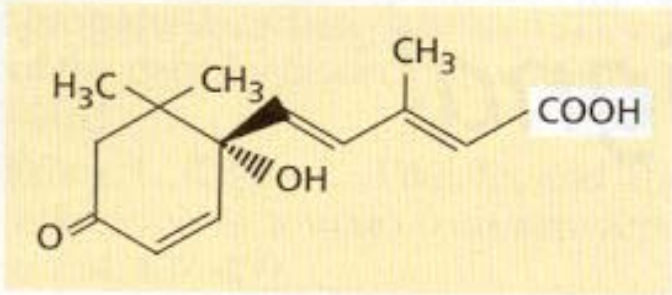

(*S*)-2-*trans*-ABA (inactive, but interconvertible with active [*cis*] form)

FIGURE 23.1 The chemical structures of the *S* (counterclockwise array) and *R* (clockwise array) forms of *cis*-ABA, and the (*S*)-2-*trans* form of ABA. The numbers in the diagram of (*S*)-*cis*-ABA identify the carbon atoms.

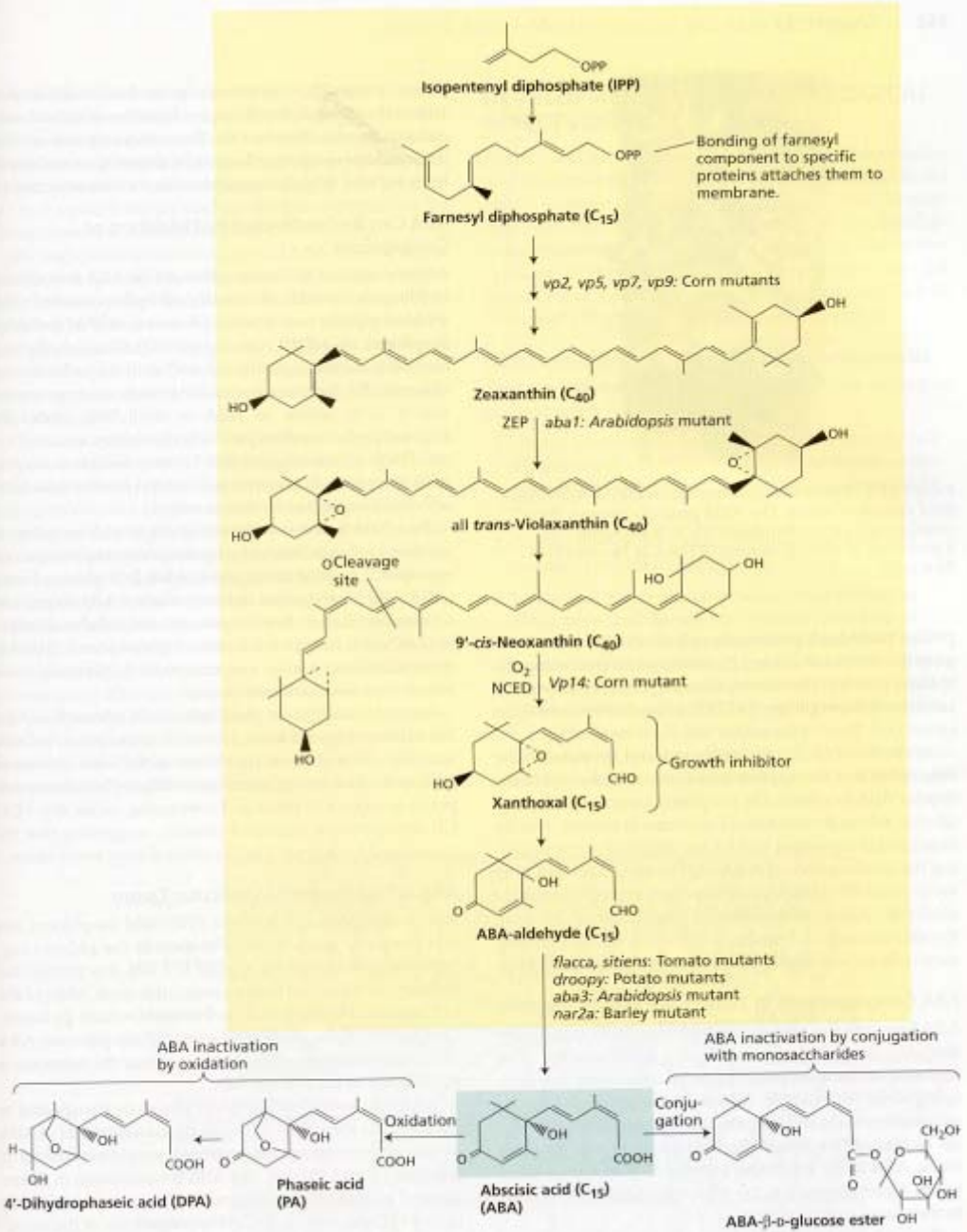

FIGURE 23.2 ABA biosynthesis and metabolism. In higher plants, ABA is synthesized via the terpenoid pathway (see Chapter 13). Some ABA-deficient mutants that have been helpful in elucidating the pathway are shown at the steps at which they are blocked. The pathways for ABA catabolism include conjugation to form ABA-β-D-glucosyl ester or oxidation to form phaseic acid and then dihydrophaseic acid. ZEP = zeaxanthin epoxidase; NCED = 9-cis-epoxycarotenoids dioxygenase.

FIGURE 23.3 Precocious germination in the ABA-deficient *vp14* mutant of maize. The VP14 protein catalyzes the cleavage of 9-*cis*-epoxycarotenoids to form xanthoxal, a precursor of ABA. (Courtesy of Bao Cai Tan and Don McCarty.)

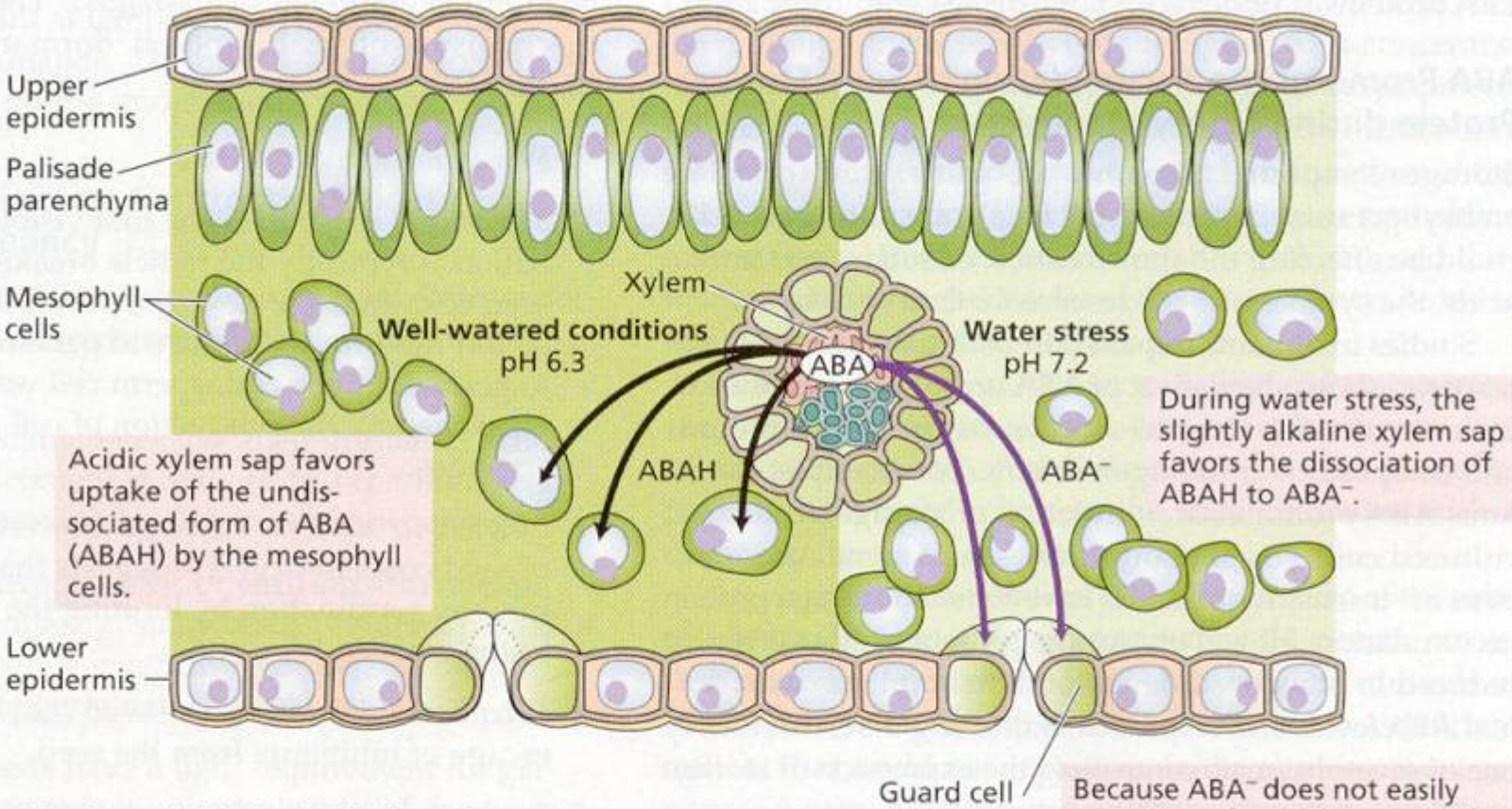

FIGURE 23.4 Redistribution of ABA in the leaf resulting from alkalinization of the xylem sap during water stress.

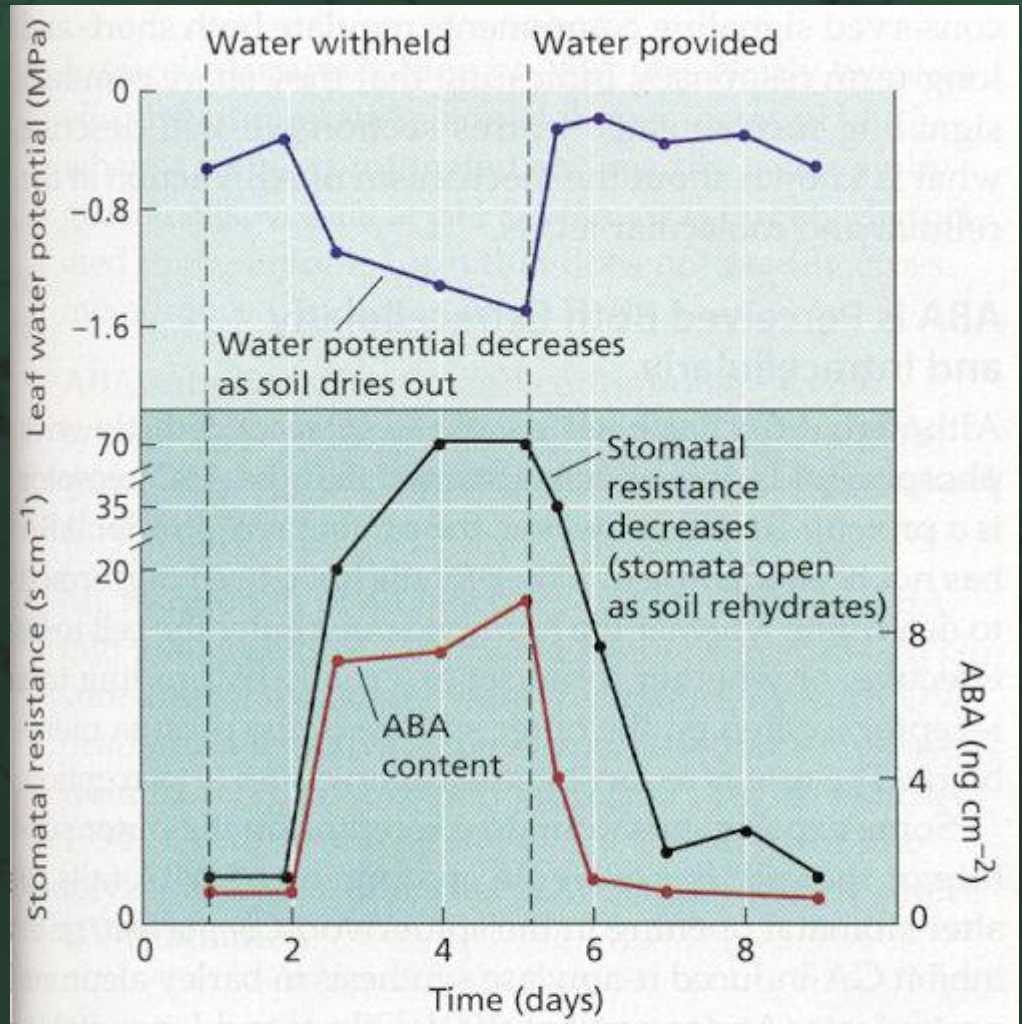

FIGURE 23.5 Changes in water potential, stomatal resistance (the inverse of stomatal conductance), and ABA content in maize in response to water stress. As the soil dried out, the water potential of the leaf decreased, and the ABA content and stomatal resistance increased. The process was reversed by rewatering. (After Beardsell and Cohen 1975.)

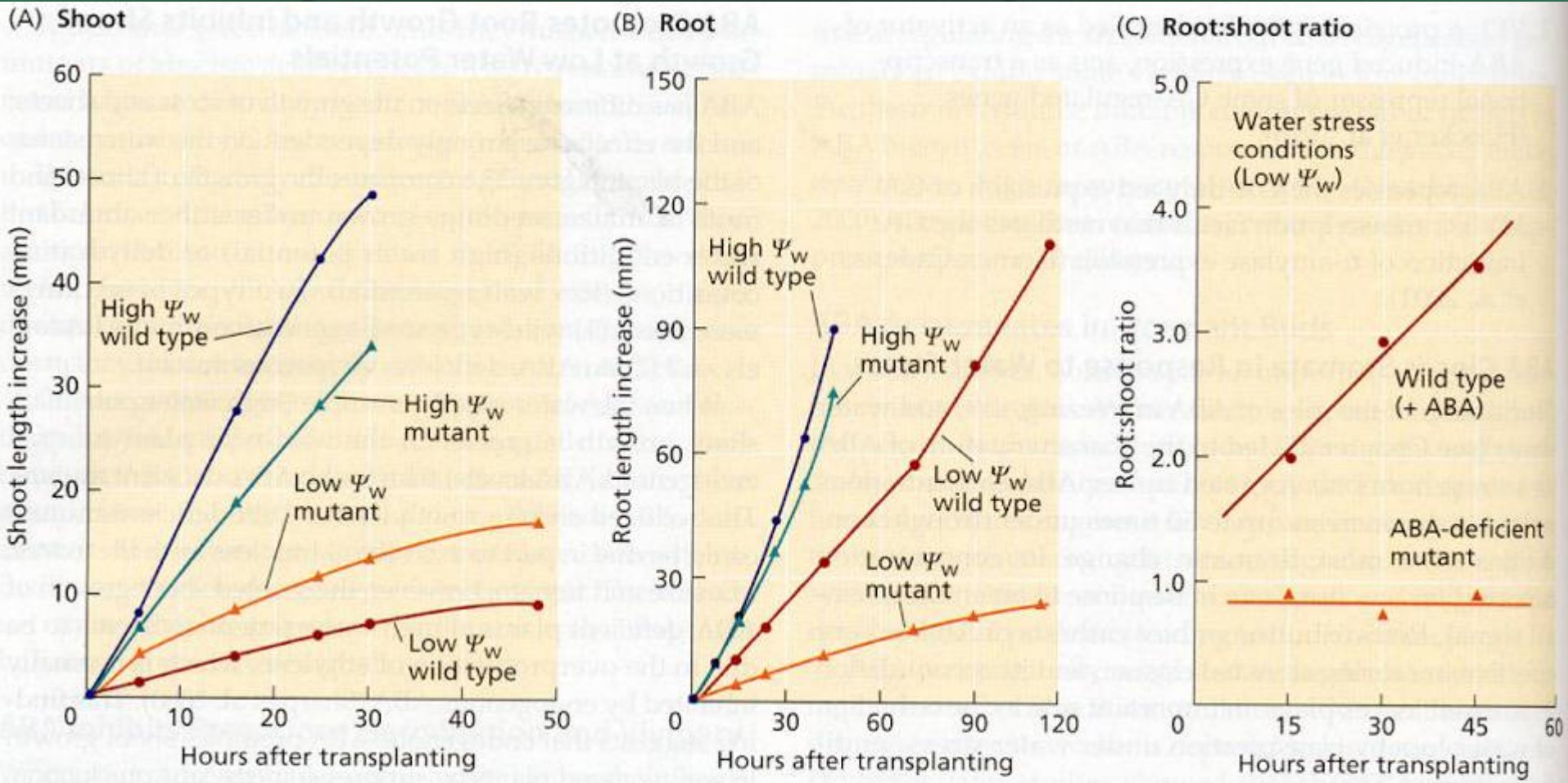

FIGURE 23.6 Comparison of the growth of the shoots (A) and roots (B) of normal versus ABA-deficient (viviparous) maize plants growing in vermiculite maintained either at high water potential (–0.03 MPa) or at low water potential (–0.3 Mpa in A and –1.6 MPa in B). Water stress (low water potential) depresses the growth of both shoots and roots compared to the controls. (C) Note that under water stress conditions (low Ψ_w), the ratio of root growth to shoot growth is much higher when ABA is present (i.e., in the wild type) than when it is absent (in the mutant). (From Saab et al. 1990.)

(A)

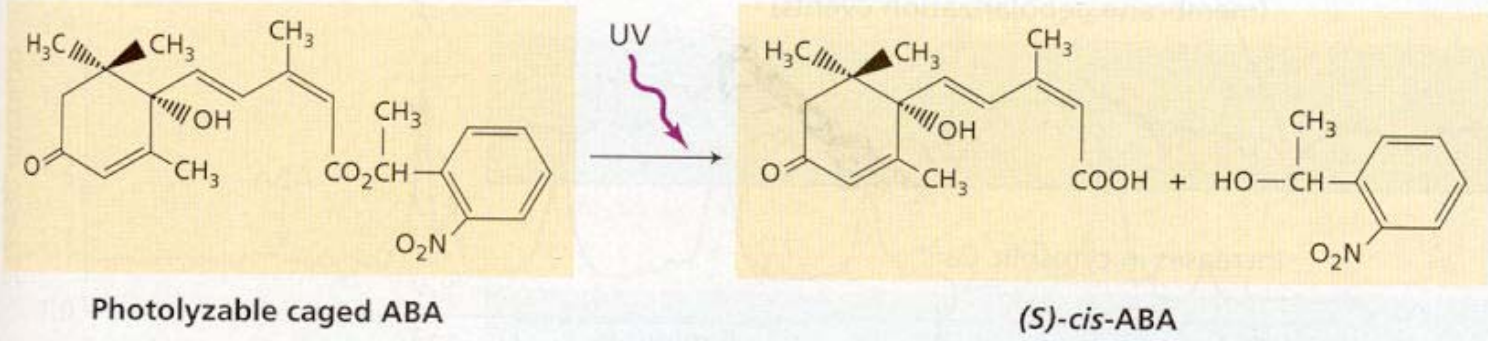

Photolyzable caged ABA

(S)-cis-ABA

(B)

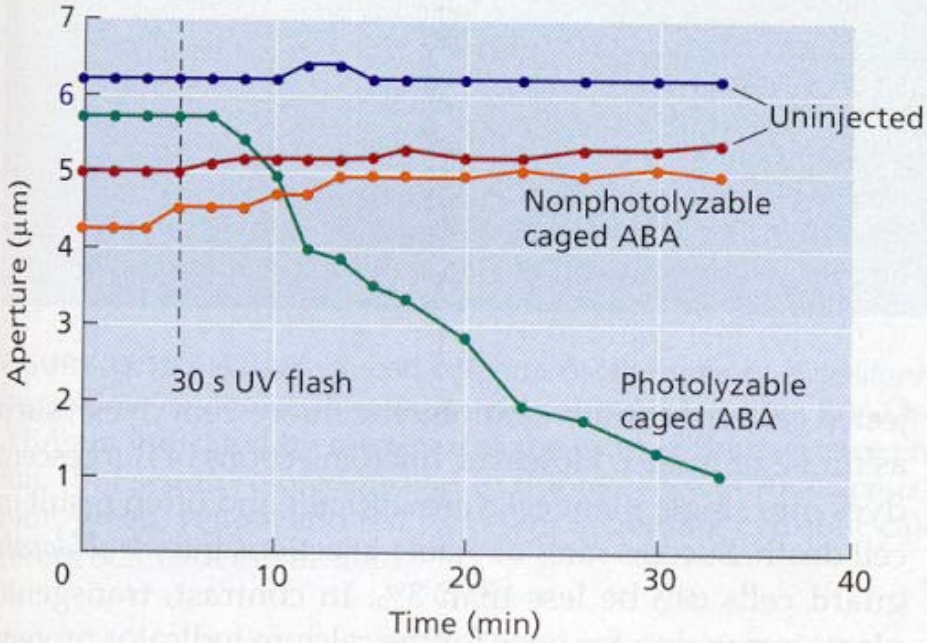

(C)

(D)

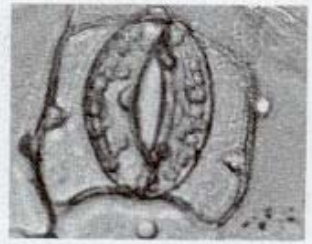

FIGURE 23.7 Stomatal closure induced by UV photolysis of caged ABA in the guard cell cytoplasm. Single guard cells in stomatal complexes of *Commelina* were microinjected with caged ABA. (A) Photolysis reaction induced by UV irradiation. (B) The stomatal apertures recorded before and after a 30-second exposure of the cells to UV. (C, D) Light micrographs of the same stomatal complex in which the right-hand guard cell was loaded with the photolyzable cages ABA 10 minutes before UV photolysis (C) and 30 minutes after photolysis (D). (A and B from Allen et al. 1994; C and D courtesy of A. Allan, from Allan et al. 1994; © American Society of Plant Biologists, reprinted with permission.)

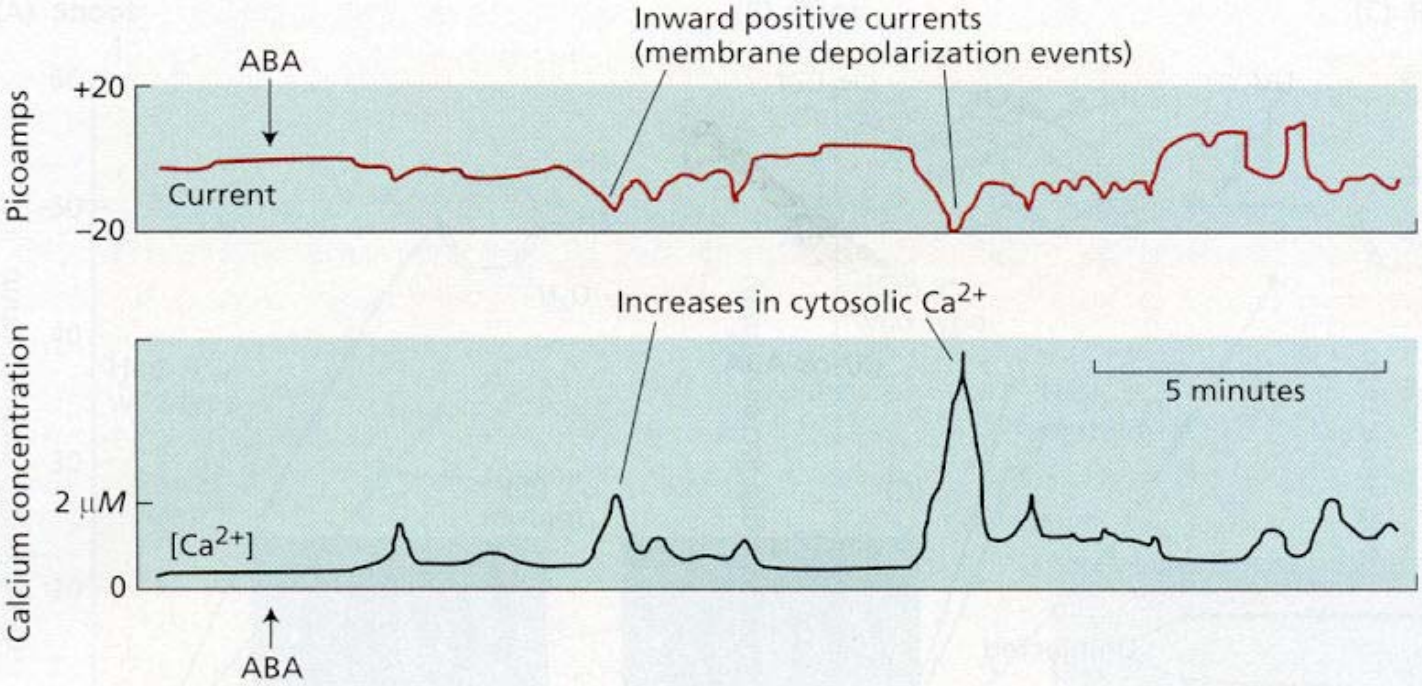

The increases in cytoplasmic Ca^{2+} roughly coincide with the membrane depolarization events.

FIGURE 23.8 Simultaneous measurements of ABA-induced inward positive currents and ABA-induced increases in cytosolic Ca^{2+} concentrations in a guard cell of *Vicia faba* (broad bean). The current was measured by the patch clamp technique; calcium was measured by use of a fluorescent indicator dye. ABA was added to the system at the arrow in each case. (From Schroeder and Hagiwara 1990.)

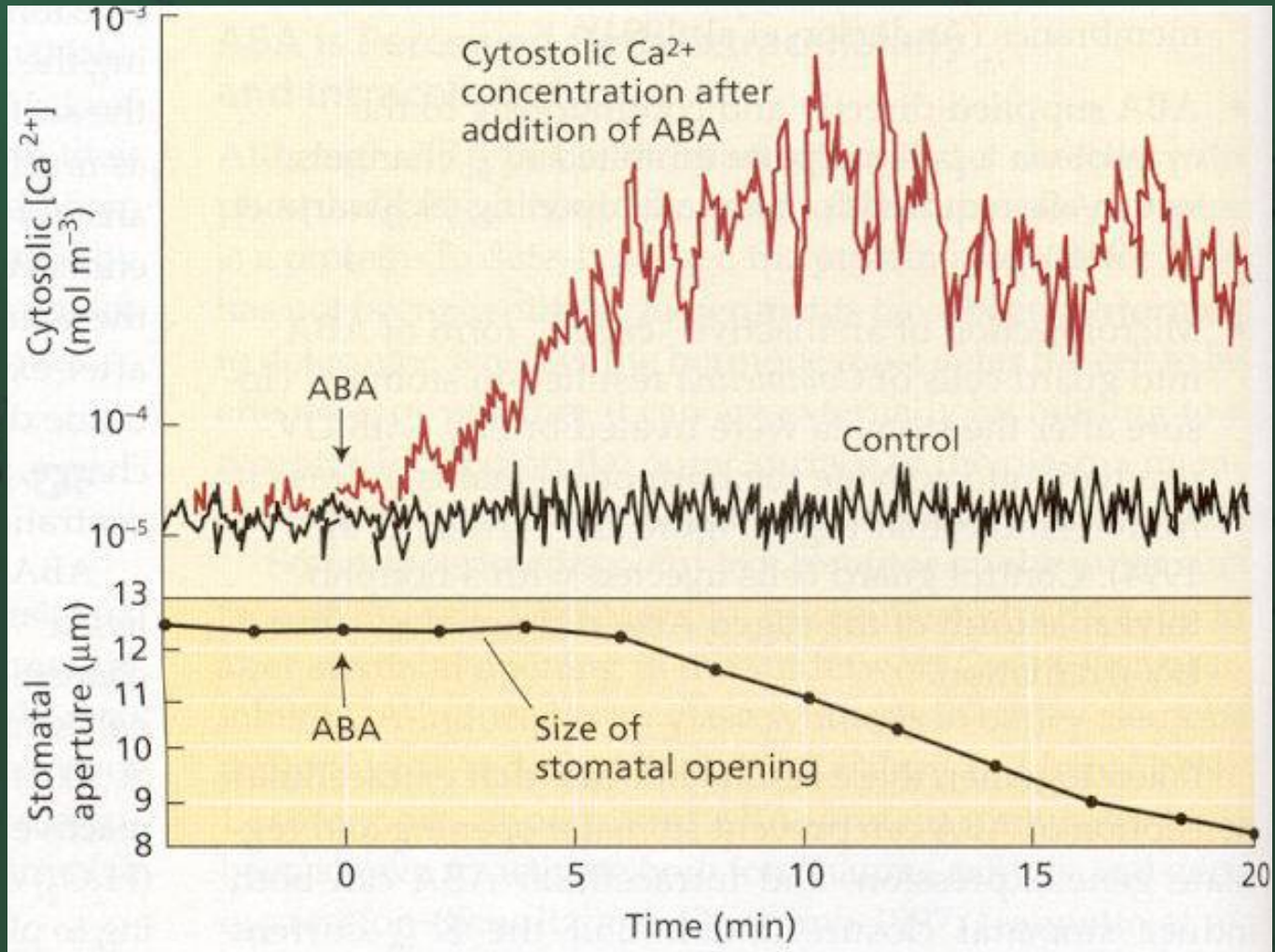

FIGURE 23.9 Time course of the ABA-induced increase in guard cell cytosolic Ca^{2+} concentration (upper panel) and ABA-induced stomatal aperture (lower panel). (From Mansfield and McAinsh 1995.)

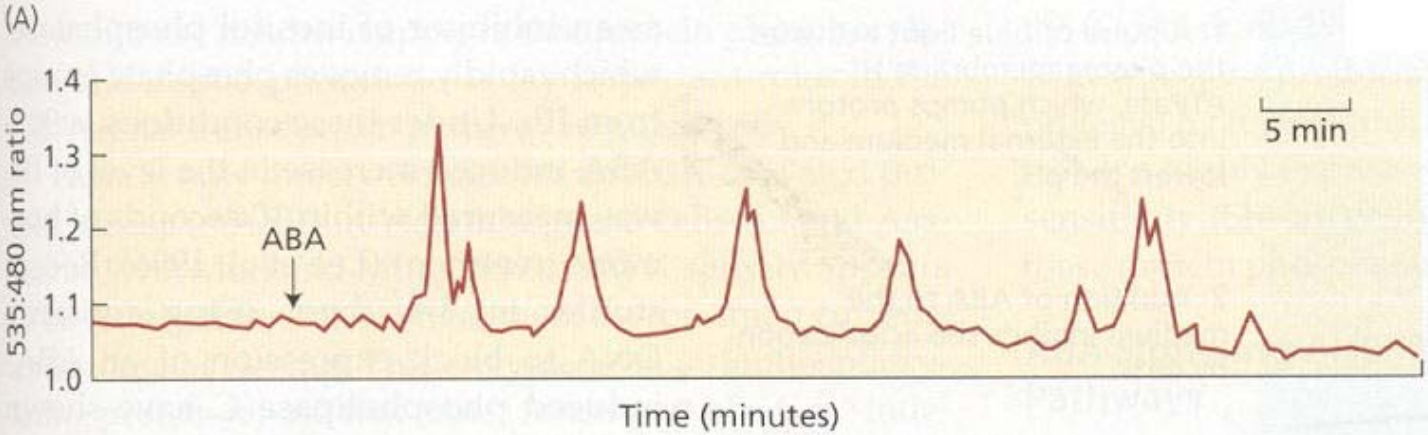

(B)

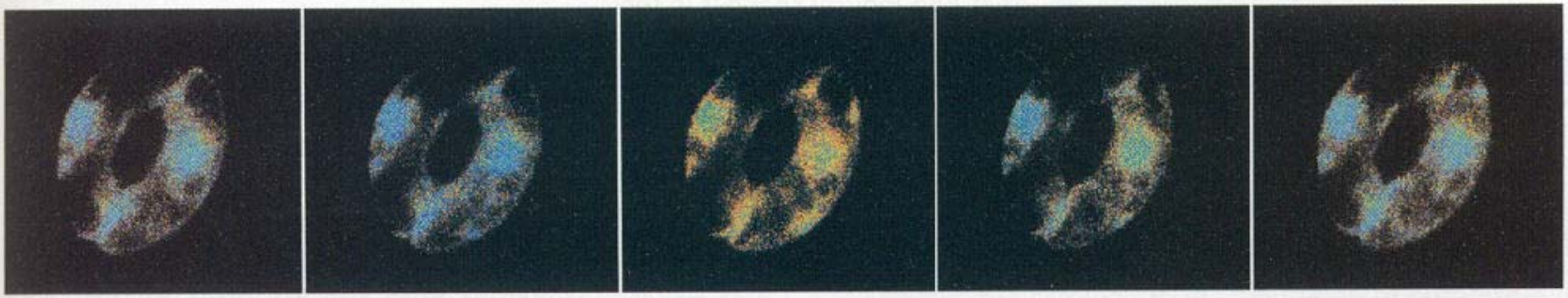

FIGURE 23.10 ABA-induced calcium oscillations in *Arabidopsis* guard cells expressing yellow cameleon, a calcium indicator protein dye. (A) Oscillations elicited by ABA are indicated by increases in the ratio of flourescence emission at 535 and 480 nm. (B) Pseudo colored images of fluorescence in *Arabidopsis* guard cells, where blue, green, yellow and red represent increasing cytosolic calcium concentration. (From Schroeder et al. 2001.)

1. ABA binds to its receptors.

2. ABA-binding induces the formation of reactive oxygen species, which activate plasma membrane Ca^{2+} channels.

3. ABA increases the levels of cyclic ADP-ribose and IP_3, which activate additional calcium channels on the tonoplast.

4. The influx of calcium initiates intracellular calcium oscillations and promotes the further release of calcium from vacuoles.

5. The rise in intracellular calcium blocks K^+_{in} channels.

6. The rise in intracellular calcium promotes the opening if Cl^-_{out} (anion) channels on the plasma membrane, causing membrane depolarization.

7. The plasma membrane proton pump is inhibited by the ABA-induced increase in cytostolic calcium and a rise in intracellular pH, further depolarizing the membrane.

8. Membrane depolarization activates K^+_{out} channels.

9. K^+ and anions to be released across the plasma membrane are first released from vacuoles into the cytosol.

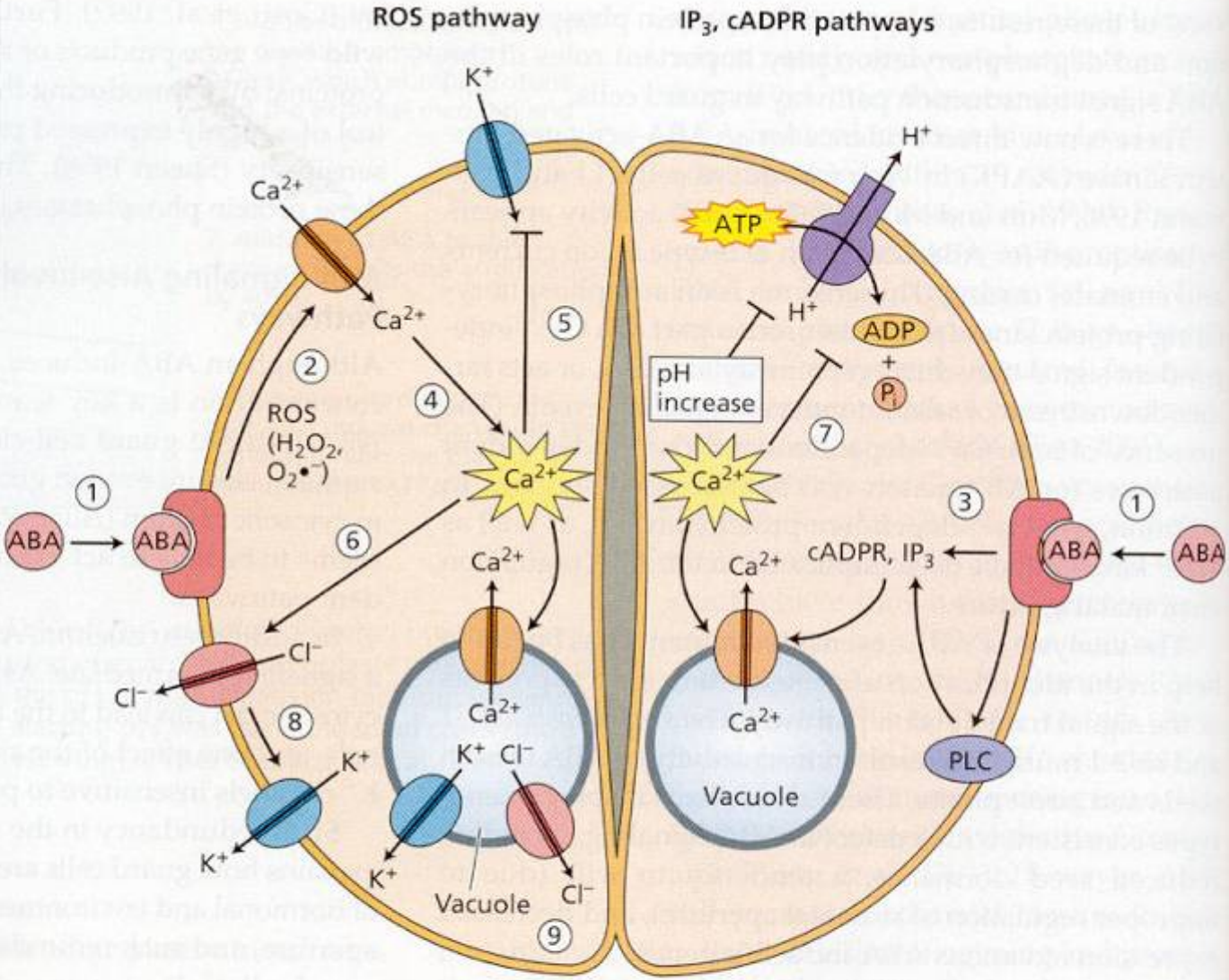

FIGURE 23.12 Simplified model for ABA signaling in stomatal guard cells. The net effect is the loss of potassium and its anion (Cl^- or malate^{2-}) from the cell. (R = receptor; ROS = reactive oxygen species; cADPR = cyclic ADP-ribose; G-protein = GTP-binding protein; PLC = phospholipiase C.)